



Metal-Catechol Network (MCN) Based Bioactive Surface Engineering of Iron Reinforced Hydroxyapatite Nanorods for Bone Tissue Engineering [†]

Zahid Hussain ^{1,2} , Ismat Ullah ² , Zhuangzhuang Zhang ^{1,2} and Renjun Pei ^{1,2,*}

¹ School of Nano-Tech and Nano-Bionics, University of Science and Technology of China (USTC), Hefei 230026, China; zahid@mail.ustc.edu.cn (Z.H.); zzzhang2021@sinano.ac.cn (Z.Z.)

² CAS Key Laboratory for Nano-Bio Interface, Division of Nanobiomedicine, Suzhou Institute of Nano-Tech and Nano-Bionics, Chinese Academy of Sciences, Suzhou 215123, China; ullah2020@sinano.ac.cn

* Correspondence: rjpei2011@sinano.ac.cn

[†] Presented at the 3rd International Online-Conference on Nanomaterials, 25 April–10 May 2022; Available online: <https://iocn2022.sciforum.net/>.

Abstract: Hydroxyapatite (HAp) is a calcium phosphate-based inorganic constitute in bones and teeth. The synthesis of nanostructured rods that mimic the natural bone apatite has attracted significant attention. Unfortunately, pristine HAp is unsuitable for clinical translation due to its brittleness, limited strength, uncontrolled leaching, and poor surface properties. These limitations necessitate size reduction, surface modification, and ion incorporation to expand their scope in bone reconstruction. Herein, iron-reinforced hydroxyapatite nanorods (Fe-HAp) were used as an inorganic component, and catechol-modified gelatin methacryloyl was employed as a surface functional modifier agent. Our study highlighted that Fe-doped HAp nanomaterials are more promising for developing bioactive surfaces than other ion-incorporated nanomaterials due to their metal-catechol network (MCN) surface engineering. Nanostructural, surface chemistries, cytocompatibility, and matrix mineralization characteristics of Fe-HAp and Fe-HAp/MCN nanorods have been comparatively studied. The results support that MCN-coated nanorod surfaces improved HAp cytocompatibility, bioactivity, and phase compatibility between organic/inorganic nanomaterials, which could be crucial for bone reconstruction.

Keywords: hydroxyapatite nanorods; metal-catechol network; organic/inorganic composites; biointerface; bone tissue engineering



Citation: Hussain, Z.; Ullah, I.; Zhang, Z.; Pei, R. Metal-Catechol Network (MCN) Based Bioactive Surface Engineering of Iron Reinforced Hydroxyapatite Nanorods for Bone Tissue Engineering. *Mater. Proc.* **2022**, *9*, 16. <https://doi.org/10.3390/materproc2022009016>

Academic Editor: Eleonore Fröhlich

Published: 22 April 2022

Publisher's Note: MDPI stays neutral with regard to jurisdictional claims in published maps and institutional affiliations.



Copyright: © 2022 by the authors. Licensee MDPI, Basel, Switzerland. This article is an open access article distributed under the terms and conditions of the Creative Commons Attribution (CC BY) license (<https://creativecommons.org/licenses/by/4.0/>).

1. Introduction

Bone is an inorganic-organic composite. It comprises ~70% inorganic materials and ~30% organic biomolecules. The organic molecules provide a softer matrix while the inorganic matrix hardens the bone structure [1,2]. The unprecedented aging of the world's population and the growing prevalence of age-related conditions, such as osteoporosis and bone fractures, boosted the need for bioengineering strategies to repair complicated bone defects [3,4]. In recent years, hydroxyapatite (HAp), halloysite nanotube, glass nanoparticles, etc., have been increasingly recognized for their potential for bone reconstruction. Hydroxyapatite (HAp) is the main calcium phosphate-based inorganic component that is present in the matrix of bone. The synthesis of the nanostructured HAp rod that recapitulates bone-apatite properties has attracted significant research interest [5,6]. HAp nanoscale rods have been employed for surface coating of bone/dental implants, delivery of bioactive biomolecules, and graft replacement due to their osteoconduction, osteoblast maturation, and osteointegration properties [7,8]. Many studies agreed that using pristine HAp rods is not beneficial for bone repair application due to its high brittleness, low strength, and uncontrolled aggregation. Furthermore, pristine HAp nanomaterials

have few functional groups on their nanoscale surface and, therefore, exhibit weak phase compatibility between inorganic/organic matrices [9,10]. These shortcomings necessitate HAp surface modification, ion integration into HAp lattice, and polymeric surface coating, which could broaden their scope in bone bioengineering [11,12]. Herein, catechol-modified gelatin methacryloyl (GelMA-C) was coated on the surface of Fe-HAp nanorods using a metal-catechol network (MCN). Our study highlighted that Fe-doped HAp was more promising for constructing bioactive organic interfaces and increasing interface interaction between inorganic/organic matrix than other ion-doped nanorods. The nanostructural, surface chemistries, cytocompatibility, and matrix mineralization characteristics of Fe-HAp nanorods and Fe-HAp/MCN nanorods (or inorganic/organic) have been comparatively studied. The results support that MCN-coated nanorod surfaces better regulate interface interactions, cytocompatibility, the fusion between organic/inorganic nanomaterials, and matrix production, which are crucial for compromised bone reconstruction.

2. Material and Methods

2.1. Materials

Methacrylic anhydride, ferric chloride hexahydrate ($\text{FeCl}_3 \cdot 6\text{H}_2\text{O}$), porcine skin-derived gelatin type A, calcium nitrate tetrahydrate, ammonia solution, and diammonium hydrogen phosphate were used in nanorods synthesis and their surface modification. MC3T3-E1 cells, alpha-MEM (α MEM), Fetal bovine serum (FBS), trypsin-EDTA (0.25%), penicillin-streptomycin solution, and phosphate buffer saline (PBS) were used in cell culture experiments. Live/Dead[®] reagent and BCIP/NBT ALP kit were used in biochemical assays.

2.2. Synthesis of Fe-HAp/MCN Nanorods

Iron doped HAp were synthesized via aqueous precipitation followed by the sonification method according to our previously discussed protocol [13,14]. Gelatin methacryloyl (GelMA) is synthesized by adding methacrylate groups to lysine groups of peptide chains of gelatins and further modified with catechol moieties. The resultant polymeric product was termed catechol-modified GelMA (GelMA-C). The coating of Fe doped HAp with GelMA-C has performed in 2.5% acetic acids at 10:1 (*w/w*) ratio under continuous stirring for 5 h at 37 °C. After the surface engineering reaction, the solid precipitate was washed to remove unbounded, unreacted, and excess GelMA-C via three times centrifugation at 4000 rpm for 8 min with deionized water. Polymer-coated Fe-HAp (Fe-HAp/MCN) was freeze-dried for 36 h. The obtained powder was stored at room temperature −4 °C.

2.3. Characterization of Fe-HAp/MCN Nanorods

The colorimetric change in nanorods powder before and after surface modification was noticed using a mobile camera. The Fe-HAp and Fe-HAp/MCN nanorods' nanostructural characteristics were investigated under a transmission electron microscope (TEM, HT7700). The diameters and shape factors ($n = 30$) of nanomaterials from TEM images were determined using the ImageJ program. The element composition and elemental mapping of Fe-HAp and modified HAp nanorods were studied under energy-dispersive X-ray spectroscopy (EDS, Oxford Instruments). MC3T3-E1 cells were cultured in α MEM + 10% FBS + 1% double antibiotic medium in 5% CO_2 incubator. The confluent MC3T3-E1 cells (80%) were rinsed, trypsinized using 0.25% trypsin with EDTA, centrifuge at 1000 rpm for 3 min, resuspended to get desired cell concentration (2.5×10^4), and spread in plate wells for further assays. The cultured cells were separately treated with $55 \mu\text{g mL}^{-1}$ Fe-HAp, and $55 \mu\text{g mL}^{-1}$ Fe-HAp/MCN for up to 3 d. The nanorods treated MC3T3-E1 (after 72 h of incubation) were incubated at room temperature for 50 min in a 300 μL FBS free fresh medium containing 8 μL calcein dye (stain live cells) and 8 μL propidium iodide dye (stain dead cells). The dye-treated samples were rinsed five times with PBS and imaged under the confocal microscope to study the percentage of live and dead cells. The nanorods treated MC3T3-E1 were washed, fixed, and stained with BCIP/NBT dye following manufacturer guidelines after 10 d of incubation, and resultant stained samples were studied under a

compound microscope. All experiments were performed at least three times unless mentioned differently. Qualitative investigations were conducted under identical instrument settings, and representative micrographs were shown. Quantitative experimental data were expressed as \pm standard deviations (SD).

3. Results and Discussion

Fe ions are required for cellular growth. Our previous research has shown that incorporating ions into the nanorods lattice lowers crystallinity and increases HAp bioactive properties. Ion-doped HAp boosted matrix mineralization and osseointegration activity of cells compared to ion-free inorganic nanorods [13,14]. The pristine HAp nanorods possess few functional groups, offer limited fusion interaction between organic/inorganic matrix, and hold poor bioactivity [15]. The Fe-doped nanomaterials are more promising for creating functional interfaces than other ion-doped nanomaterials due to supramolecular MCN surface engineering [16]. The GeLMA-C is appealing for numerous reasons, such as high cell-binding arginine-glycine-aspartic acid motifs, matrix-metalloproteinase mediated degradability, hold poor immunogenicity [17]. The GeLMA-C nanoscale coating changes the colorimetric properties of Fe-doped HAp from yellow to light-dark, demonstrating supramolecular interaction between GeLMA-C and Fe^{3+} doped HAp, and confirmed successful MCN formation (Figure 1A). TEM showed that Fe-HAp exhibited rod structure with a consistent width of 16 ± 04 nm and about lengths 70 ± 09 nm. GeLMA-C increases the diameter of nanorods in the nanoscale range, indicating the single-layer modification ($\sim 14 \pm 03$ nm). The structural and shape factor characteristics of polymeric-modified nanorods (width, ~ 25 nm; length, ~ 88 nm) resemble bone apatite rod-shaped structures (Figure 1B). EDS-based elemental data and elemental mapping results indicated that nitrogen (N) and carbon (C) content significantly increased in Fe-HAp/MCN compared to Fe-HAp nanorod mainly due to MCN surface modification (Figure 1C,D).

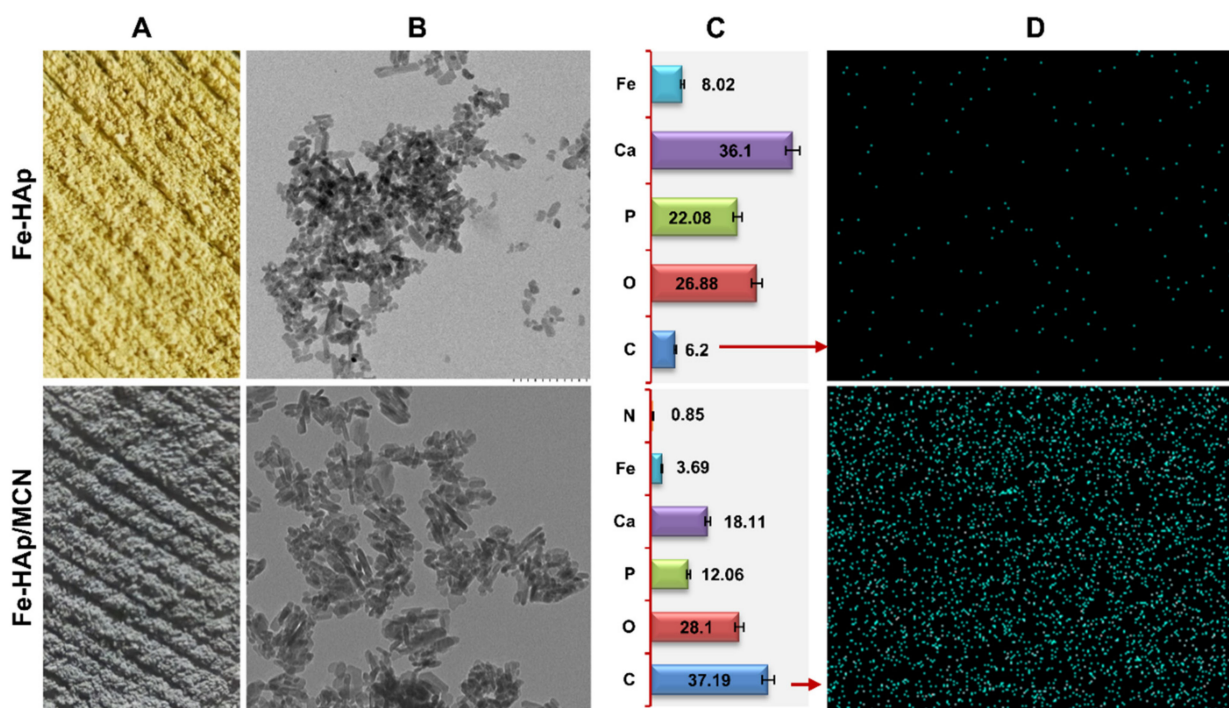


Figure 1. (A) Colorimetric morphology of Fe doped HAp nanorods and Fe-HAp/MCN nanorods powder. (B) TEM-based microscopic morphology of Fe doped HAp nanorods and Fe-HAp/MCN nanorods. Scale bar, 200 nm. (C) The EDS-based atomic percentage of various elements present in Fe doped HAp nanorods and Fe-HAp/MCN nanorods. (D) EDS mapping of elements present in Fe-HAp nanorods and Fe-HAp/MCN nanorods.

MCN coating is a simple approach that did not require any special equipment, does not involve harmful chemical reagents, and generates repeatable nanocoating on the Fe-HAp surface [18]. Various investigations have demonstrated the pH-stimulated role of MCN and depicted that catechol-iron mono-network generated at pH less than 2, bis-network generated at a pH between 2 and 6, and tris-network can be generated at pH around 6–7. Since Fe was doped into the lattice of HAp nanorods, only a few functional sites were available on the nanorod's surface for interface complexation with catechol moieties. Thus, a 1:1 catechol: Fe^{3+} or 2:1 catechol: Fe^{3+} network could be generated onto the nanomaterial's surface. [19,20]. Since it is challenging to control physical coating at the nano level, the unique MCN coating strategy can be stabilized at the nanoscale range (less than 20 nm). The representative live/dead data showed that live-cells % was higher in modified nanorods treated cells than Fe-HAp treated cells. It supported the notion that the GeLMA-C nanoscale coating onto HAp nanorods significantly promotes their biological role (Figure 2A). The higher ALP quantity (used as an early-stage osteogenic marker) was noted on organic/inorganic nanorods treated MC3T3-E1 cells than on inorganic nanorods treated MC3T3-E1 cells. It demonstrates osteoblast maturation and higher biosynthetic properties of organic/inorganic nanorods (Figure 2B). Overall, these results demonstrated the simplicity of the iron-catechol complexation and indicated that GeLMA-C improved cytocompatibility, build functional interfaces, and could broaden the applications of organic/inorganic nanorods in bone tissue reconstruction.

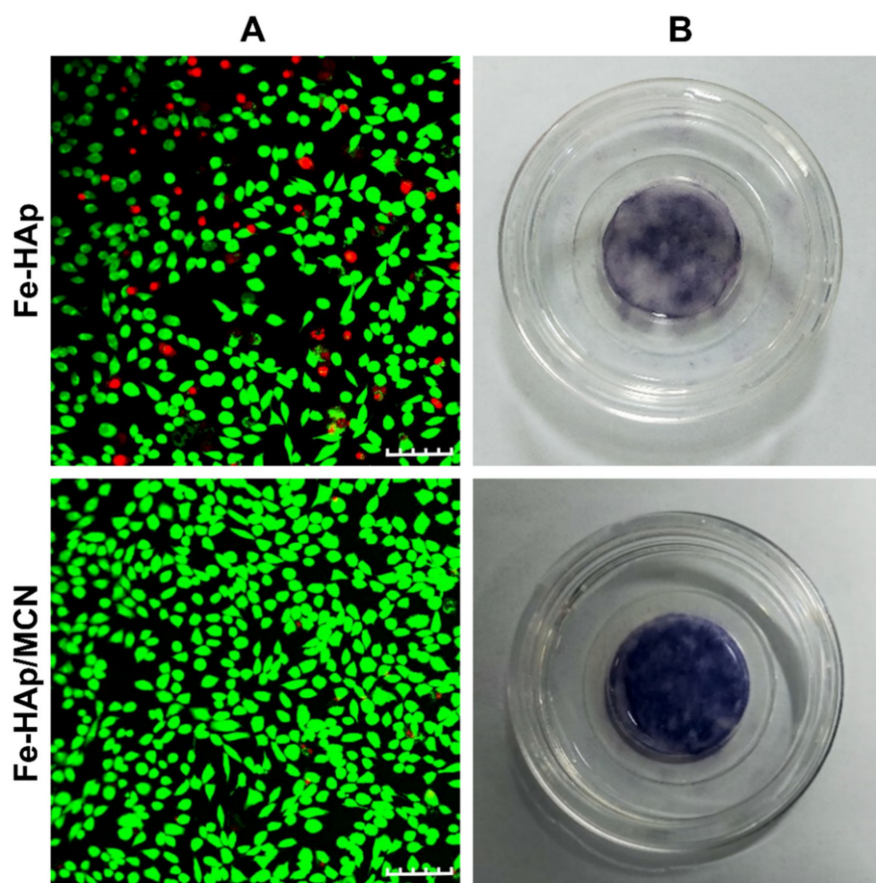


Figure 2. (A) Live cells (green fluorescent) and dead cells (red fluorescent) staining showed that MCN surface-modified nanorods increased MC3T3-E1 survivability more than Fe doped inorganic nanorods. Scale bar, 100 μm . (B) The representative photograph of ALP-stained nanorods treated MC3T3-E1 cells after 10 d of incubation showed that organic/inorganic nanorods better-promoted matrix mineralization than Fe-doped inorganic nanorods.

4. Conclusions

The significant difference in colorimetric properties, nanostructural characteristics, and elemental composition supported successful MCN nanocoating onto iron-doped HAP nanorods via metal-catechol network mechanism. MCN-based surface coating promotes fusion interfaces, cytocompatibility, improved phase compatibility, resulting in the synthesis of single-phase inorganic/organic nanorods. The organic-inorganic nanorods were critical for MC3T3-E1 matrix maturation and could enable cell differentiation for bone repair more than inorganic nanorods. Future research will address organic/inorganic nanorods' role in genuine preclinical situations using an animal model.

Author Contributions: Conceptualization, methodology, formal analysis, investigation, writing—original draft, Z.H.; methodology, validation, investigation, data curation I.U. and Z.Z.; conceptualization, supervision, resources, review and editing, project administration, funding acquisition. R.P. All authors have read and agreed to the published version of the manuscript.

Funding: This study was supported by the Strategic Priority Research Program of Chinese Academy of Sciences (XDA16040700) and the National Natural Science Foundation of China (31971326).

Institutional Review Board Statement: Not applicable.

Informed Consent Statement: Not applicable.

Data Availability Statement: Not applicable.

Acknowledgments: Z.H. is grateful to CAS-TWAS President's Ph.D. Fellowship Program.

Conflicts of Interest: The authors declare no conflict of interest.

References

1. Matsugaki, A.; Isobe, Y.; Saku, T.; Nakano, T. Quantitative regulation of bone-mimetic, oriented collagen/apatite matrix structure depends on the degree of osteoblast alignment on oriented collagen substrates. *J. Biomed. Mater. Res. A* **2015**, *103*, 489–499. [[CrossRef](#)] [[PubMed](#)]
2. Liu, Y.; Luo, D.; Wang, T. Hierarchical structures of bone and bioinspired bone tissue engineering. *Small* **2016**, *12*, 4611–4632. [[CrossRef](#)] [[PubMed](#)]
3. Bosco, R.; Edreira, E.R.U.; Wolke, J.G.; Leeuwenburgh, S.C.; van den Beucken, J.J.; Jansen, J.A. Instructive coatings for biological guidance of bone implants. *Surf. Coat. Technol.* **2013**, *223*, 91–98. [[CrossRef](#)]
4. Koons, G.L.; Diba, M.; Mikos, A.G. Materials design for bone-tissue engineering. *Nat. Rev. Mater.* **2020**, *5*, 584–603. [[CrossRef](#)]
5. Zhou, H.; Lee, J. Nanoscale hydroxyapatite particles for bone tissue engineering. *Acta Biomater.* **2011**, *7*, 2769–2781. [[CrossRef](#)] [[PubMed](#)]
6. Singh, G.; Singh, R.P.; Jolly, S.S. Customized hydroxyapatites for bone-tissue engineering and drug delivery applications: A review. *J. Solgel. Sci. Technol.* **2020**, *94*, 505–530. [[CrossRef](#)]
7. Lowe, B.; Hardy, J.G.; Walsh, L.J. Optimizing nanohydroxyapatite nanocomposites for bone tissue engineering. *ACS Omega* **2019**, *5*, 1–9. [[CrossRef](#)]
8. Ramesh, N.; Moratti, S.C.; Dias, G.J. Hydroxyapatite–polymer biocomposites for bone regeneration: A review of current trends. *J. Biomed. Mater. Res. Part B Appl. Biomater.* **2018**, *106*, 2046–2057. [[CrossRef](#)] [[PubMed](#)]
9. Zakaria, S.M.; Sharif Zein, S.H.; Othman, M.R.; Yang, F.; Jansen, J.A. Nanophase hydroxyapatite as a biomaterial in advanced hard tissue engineering: A review. *Tissue Eng. Part B Rev.* **2013**, *19*, 431–441. [[CrossRef](#)] [[PubMed](#)]
10. Ressler, A.; Žužić, A.; Ivanišević, I.; Kamboj, N.; Ivanković, H. Ionic substituted hydroxyapatite for bone regeneration applications: A review. *Open Ceram.* **2021**, *6*, 100122. [[CrossRef](#)]
11. Arcos, D.; Vallet-Regí, M. Substituted hydroxyapatite coatings of bone implants. *J. Mater. Chem. B* **2020**, *8*, 1781–1800. [[CrossRef](#)] [[PubMed](#)]
12. Mansoorianfar, M.; Mansourianfar, M.; Fathi, M.; Bonakdar, S.; Ebrahimi, M.; Zahrani, E.M.; Hojjati-Najafabadi, A.; Li, D. Surface modification of orthopedic implants by optimized fluorine-substituted hydroxyapatite coating: Enhancing corrosion behavior and cell function. *Ceram. Int.* **2020**, *46*, 2139–2146. [[CrossRef](#)]
13. Ullah, I.; Li, W.; Lei, S.; Zhang, Y.; Zhang, W.; Farooq, U.; Ullah, S.; Ullah, M.W.; Zhang, X. Simultaneous co-substitution of $\text{Sr}^{2+}/\text{Fe}^{3+}$ in hydroxyapatite nanoparticles for potential biomedical applications. *Ceram. Int.* **2018**, *44*, 21338–21348. [[CrossRef](#)]
14. Ullah, I.; Gloria, A.; Zhang, W.; Ullah, M.W.; Wu, B.; Li, W.; Domingos, M.; Zhang, X. Synthesis and characterization of sintered Sr/Fe-modified hydroxyapatite bioceramics for bone tissue engineering applications. *ACS Biomater. Sci. Eng.* **2019**, *6*, 375–388. [[CrossRef](#)] [[PubMed](#)]

15. Ullah, I.; Zhang, W.; Yang, L.; Ullah, M.W.; Atta, O.M.; Khan, S.; Wu, B.; Wu, T.; Zhang, X. Impact of structural features of Sr/Fe co-doped HAp on the osteoblast proliferation and osteogenic differentiation for its application as a bone substitute. *Mater. Sci. Eng. C* **2020**, *110*, 110633. [[CrossRef](#)]
16. Hussain, Z.; Ullah, I.; Liu, X.; Shen, W.; Ding, P.; Zhang, Y.; Gao, T.; Mansoorianfar, M.; Gao, T.; Pei, R. Tannin-reinforced iron substituted hydroxyapatite nanorods functionalized collagen-based composite nanofibrous coating as a cell-instructive bone-implant interface scaffold. *Chem. Eng. J.* **2022**, *438*, 135611. [[CrossRef](#)]
17. Costa, P.M.; Learmonth, D.A.; Gomes, D.B.; Cautela, M.P.; Oliveira, A.C.; Andrade, R.; Espregueira-Mendes, J.; Veloso, T.R.; Cunha, C.B.; Sousa, R.A. Mussel-Inspired Catechol Functionalisation as a Strategy to Enhance Biomaterial Adhesion: A Systematic Review. *Polymers* **2021**, *13*, 3317. [[CrossRef](#)] [[PubMed](#)]
18. Zhang, Y.; Shen, L.; Zhong, Q.Z.; Li, J. Metal-phenolic network coatings for engineering bioactive interfaces. *Colloids Surf. B Biointerfaces* **2021**, *205*, 111851. [[CrossRef](#)] [[PubMed](#)]
19. Guo, J.; Ping, Y.; Ejima, H.; Alt, K.; Meissner, M.; Richardson, J.J.; Yan, Y.; Peter, K.; Von Elverfeldt, D.; Hagemeyer, C.E.; et al. Engineering multifunctional capsules through the assembly of metal-phenolic networks. *Angew. Chem. Int. Ed.* **2014**, *53*, 5546–5551. [[CrossRef](#)] [[PubMed](#)]
20. Dai, Q.; Yu, Q.; Tian, Y.; Xie, X.; Song, A.; Caruso, F.; Hao, J.; Cui, J. Advancing metal-phenolic networks for visual information storage. *ACS Appl. Mater. Interfaces* **2019**, *11*, 29305–29311. [[CrossRef](#)] [[PubMed](#)]